Journal of Applied Sciences

ISSN 1812-5654

science alert

ANSInet
an open access publisher
http://ansinet.com

OPEN ACCESS Journal of Applied Sciences

ISSN 1812-5654
DOI: 10.3923/jas.2017.135.141

Research Article
Nonlinear Control of an Induction Machine using Robust Controller based on H∞ Algorithm

[1,2]Olivier Asseu, [1]Pamela Yoboue, [3]Paul Kouakou, [2]Pierre Tety and [1]Raoul Zamble

[1]Ecole Supérieure Africaine des TIC (ESATIC), Abidjan, Côte d'Ivoire
[2]Institut National Polytechnique Félix Houphouët Boigny (INP-HB), Yamoussoukro, Côte d'Ivoire
[3]Université Nangui Abrogoua, (UNA), Abidjan, Côte d'Ivoire

Abstract

Background and Objective: This study proposes a nonlinear feedback method and H∞ robust controller in order to assure a good decoupling, robustness performance and stability of the Induction Motor (IM) states. **Methodology:** By choosing the nonlinear dynamic model of the IM in a (d, q) synchronous reference frame, this study uses an input-output linearization approach and H∞ algorithm to define robust controllers in order to have a good regulation and convergence of the currents and then control independently the rotor speed and the flux. **Results:** The simulation results for a 5.5 kW induction motor are presented to illustrate the effectiveness and the high robustness of the proposed approach against parameter variations and disturbances. **Conclusion:** Thus, in the industrial applications, one will appreciate very well the use of a robust feedback decoupling strategy in order to control the currents and then preserve the robustness stability of an induction motor under disturbances.

Key words: Induction motor, nonlinear feedback control, H∞ robust control, Matlab/Simulink

Received: September 17, 2016 Accepted: December 22, 2016 Published: February 15, 2017

Citation: Olivier Asseu, Pamela Yoboue, Paul Kouakou, Pierre Tety and Raoul Zamble, 2017. Nonlinear control of an induction machine using robust controller based on H∞ algorithm. J. Applied Sci., 17: 135-141.

Corresponding Author: Olivier Asseu, Ecole Supérieure Africaine des TIC (ESATIC), Abidjan, Côte d'Ivoire Tel: (+225) 08078605

Competing Interest: The authors have declared that no competing interest exists.

Data Availability: All relevant data are within the paper and its supporting information files.

INTRODUCTION

During the last decade, the Induction Motors (IM) become more and more popular for motion control applications and widely used in industrial developments[1] due to its reasonable cost, robust qualities, simple maintenance and reliable construction. However, is proved very difficult because the dynamic model of this IM is nonlinear (due to the coupling between the electrical and mechanical state variables), multidimensional and complex where some parameters are often imprecisely known or vary with temperature, skin effect or saturation. For instance, the variation of the rotor resistance, which drifts with the temperature of the rotor current frequency can induce a lack of field orientation, a performance and stability degradation for the IM.

To guarantee good performances and stability of the IM in presence of parameters variations (resistance, inductance, etc.), it is necessary to use more elaborate control strategies. Many results have been published such as the Field Oriented Control (FOC)[2] which allows the control of the torque transient, the optimal control strategies[3] for speed control of IM drives, the robust nonlinear predictive control[4] applied to the IM for speed trajectory tracking and disturbance rejection, etc.

The naturally structure of non-linear and multivariable state of IM models induces the use of the nonlinear control methods, in particular the synthesizing of input-outputs linearization and decoupling techniques based on the Lyapunov theory[5,6]. Many manuscripts have been published in this nonlinear feedback field such as Dendouga and Abdessemed[7] and Zaidi *et al.*[8].

In this study, the feedback linearization strategy is used in order to permit a good decoupling of the IM variables in a field-oriented (d, q) coordinate so that stator currents can be separately controlled and then to control independently the generated torque (or speed) and the rotor flux.

Otherwise, to preserve and improve the reliability under parameters variation and noises injected by the inverter (which can induce a state-space "Coupling" and degradation of the system), a robust control approach has been made on the motor drives. Thus, compared to the traditional PI controllers which cannot achieve good output performance under a wide range of operating conditions, this robust control algorithm uses H∞ synthesis and "Doyle method"[9-12] to find adaptive currents correctors in order to insure performances of the inner current loop and stability of the global system with respect to parameters variations (specifically the noises and rotor time constant variations).

MATERIALS AND METHODS

This study, conducted in the Laboratory of Applied Electrical and Electronic (ESATIC and INPHB) from July, 2016 to October, 2012 by a theoretical work has been confirmed by simulations results on an induction machine.

Induction motor model: By assuming that the saturation of the magnetic parts and the hysteresis phenomenon are neglected, the dynamic model of the IM in a (d, q) synchronous reference frame can be described by a fifth-order non-linear differential equation with as state variables the stator currents (I_{ds}, I_{qs}), the rotor fluxes (Φ_{dr}, Φ_{qr}) and the rotor pulsation (ω_r) in Eq. 1:

$$\dot{x}_c = f_c(x_c)+g_c u$$

Where:

$$X_c = [\Phi_{dr}\ \Phi_{qr}\ I_{ds}\ I_{qs}\ \omega_r]^t,\ u = [\ V_{ds}\ V_{qs}\ ]^t \quad (1)$$

$$f_c(x_c) = \begin{bmatrix} -\sigma_r\Phi_{dr} + \omega_{sl}\Phi_{qr} + \sigma_r L_m I_{ds} \\ -\omega_{sl}\Phi_{dr} - \sigma_r\Phi_{qr} + \sigma_r L_m I_{qs} \\ \sigma_r\beta\Phi_{dr} + \beta\omega_r\Phi_{qr} - \lambda I_{ds} + \omega_s I_{qs} \\ -\beta\omega_r\Phi_{dr} + \beta\sigma_r\Phi_{qr} - \omega_s I_{ds} - \lambda I_{qs} \\ \left(p^2\frac{L_m}{L_r J}(\Phi_{dr}I_{qs} - \Phi_{qr}I_{ds}) - \frac{p}{J}C_r - \frac{f}{J}\omega_r\right) \end{bmatrix};\quad g_c = \begin{bmatrix} 0 & 0 \\ 0 & 0 \\ \frac{1}{\sigma L_s} & 0 \\ 0 & \frac{1}{\sigma L_s} \\ 0 & 0 \end{bmatrix}$$

$$\sigma_r = \frac{1}{T_r};\quad \lambda = \lambda(\sigma_r) = \frac{1}{\sigma}\left(\frac{1}{T_s} + (1-\sigma)\sigma_r\right);\quad \beta = \frac{1-\sigma}{\sigma L_m};\quad \sigma = 1 - \frac{L_m^{\ 2}}{L_s L_r}$$

Generally the rotor speed is measurable and its variations are slow with respect to the electrical variable dynamics[5]. Under these hypotheses the rotor speed (ω_r) may be considered as a time-varying parameter so that the electrical dynamic model of the IM can be represented as a time-varying fourth order system in Eq. 2:

$$\dot{x} = f(x)+gu \quad \text{with} \quad x = [\Phi_{dr}\ \Phi_{qr}\ I_{ds}\ I_{qs}]^t,\ u = [\ V_{ds}\ V_{qs}\ ]^t \quad (2)$$

$$f(x) = \begin{bmatrix} -\sigma_r\Phi_{dr} + \omega_{sl}\Phi_{qr} + \sigma_r L_m I_{ds} \\ -\omega_{sl}\Phi_{dr} - \sigma_r\Phi_{qr} + \sigma_r L_m I_{qs} \\ \sigma_r\beta\Phi_{dr} + \beta\omega_r\Phi_{qr} - \lambda I_{ds} + \omega_s I_{qs} \\ -\beta\omega_r\Phi_{dr} + \beta\sigma_r\Phi_{qr} - \omega_s I_{ds} - \lambda I_{qs} \end{bmatrix};\quad g = \begin{bmatrix} 0 & 0 \\ 0 & 0 \\ \frac{1}{\sigma L_s} & 0 \\ 0 & \frac{1}{\sigma L_s} \end{bmatrix}$$

The electromagnetic torque defined in terms of x is in Eq. 3:

$$C_{em} = p\frac{L_m}{L_r}\left(\Phi_{dr} I_{qs} - \Phi_{qr} I_{ds}\right) \quad (3)$$

Moreover, by choosing a rotating reference frame (d, q) so that the direction of axe d is always coincident with the direction of the rotor flux representative vector (rotor field orientation: $\Phi_{dr} = \Phi_r$ = constant; $\Phi_{qr} = 0$), the dynamic model of the IM can be rewritten as in Eq. 4:

$$\dot{x} = f_r(x_r) + g.u$$

Where:

$$x_r = [\Phi_r \; I_{ds} \; I_{qs}]^t \quad (4)$$

$$f_r(x_r) = \begin{bmatrix} -\sigma_r \Phi_{dr} + \sigma_r L_m I_{ds} \\ \sigma_r \beta \Phi_{dr} - \lambda I_{ds} + \omega_s I_{qs} \\ -\beta \omega_r \Phi_{dr} - \omega_s I_{ds} - \lambda I_{qs} \end{bmatrix}; \quad g_r = \begin{bmatrix} 0 & 0 \\ \frac{1}{\sigma L_s} & 0 \\ 0 & \frac{1}{\sigma L_s} \end{bmatrix}$$

$$y = [y_1, y_2] = [h_1(x) \; h_2(x)]^t = [I_{ds} \; I_{qs}]^t$$

From this Eq. 4, it can be seen that the dynamic model of the IM can be represented as a non-linear function of the rotor time constant (σ_r). A variation of this parameter can induce, for the IM, a lack of field orientation and performance. Also, there is a strong coupling of the stator currents (I_{ds} and I_{qs}). Therefore, to determine a state feedback control law in order to completely linearize the system and decouple the currents such as the control of the current I_{qs} does not act on the behavior of I_{ds} under parameters variation and disturbances.

Decoupling feedback control of the induction machine: To analyze the synthesis of feedback control for the nonlinear dynamic model of the IM given by the system Eq. 4. The linearization condition for checking whether a nonlinear system accepts an input-output linearization is the order of the system relative degree[5]. Thus, the successive derivatives of the system outputs are given by Eq. 5:

$$\begin{cases} \dot{y}_1 = \dot{I}_{ds} = \beta\sigma_r\Phi_r - \lambda I_{ds} + \omega_s I_{qs} + \dfrac{V_{ds}}{\sigma L_s} \\ = L_f h_1(x) + L_g h_1(x) V_{ds} = \alpha_1(x) + \beta_1(x) V_{ds} \\ \dot{y}_2 = \dot{I}_{qs} = \beta\omega_r\Phi_r - \omega_s I_{ds} - \lambda I_{qs} + \dfrac{V_{ds}}{\sigma L_s} \\ = L_f h_2(x) + L_g h_2(x) V_{qs} = \alpha_2(x) + \beta_2(x) V_{qs} \end{cases} \quad (5)$$

It can be seen that the two outputs derivatives involve the inputs. Thus, the system Eq. 4 has relative degree r =2 (with $r = r_1 + r_2 = 2$) and can be transformed into a linear, decoupled and controllable system by chosen[5,6]:

- A suitable change of coordinates $z = [z_1 z_2]$ given by Eq. 6:

$$z_1 = h_1(x); \; z_2 = h_2(x) \;\; \text{with } \dot{z}_1 = v_1, \; \dot{z}_2 = v_2 \quad (6)$$

where, $[v_1, v_2]^T$ are the new input vector of the obtained decoupled systems.

- And the feedback linearization control, $U = [V_{ds} \; V_{qs}]^t$, having the following form Eq. 7:

$$u = \begin{bmatrix} L_{g_1} h_1(x) & 0 \\ 0 & L_{g_2} h_2(x) \end{bmatrix}^{-1} \cdot \begin{bmatrix} v_1 - L_{f_1} h_1(x) \\ v_2 - L_{f_2} h_2(x) \end{bmatrix} = \Delta^{-1}(x) \begin{bmatrix} v_1 - L_{f_1} h_1(x) \\ v_2 - L_{f_2} h_2(x) \end{bmatrix} \quad \text{with} \quad \Delta(x) = \begin{bmatrix} \frac{1}{\sigma.L_s} & 0 \\ 0 & \frac{1}{\sigma.L_s} \end{bmatrix} \quad (7)$$

Equation 7 is rearranged into Eq. 8:

$$\begin{cases} V_{ds} = \sigma.L_s[v_1 - (\beta.\sigma_r.\Phi_r - \lambda.I_{ds} + \omega_s.I_{qs})] \\ V_{qs} = \sigma.L_s[v_2 - (-\beta.\omega_r.\Phi_r - \omega.I_{ds} + \omega_s.I_{qs})] \end{cases} \quad (8)$$

The Jacobian matrix of the transformation Δ(x) is nonsingular for all x. The linearizing feedback control law Eq. 8 is effective and leads the system Eq. 4 in two decoupled subsystems, each one is composed of an integrator (Fig. 1). The new inputs of the obtained decoupled systems are v_1 and v_2.

The new inputs $[v_1, v_2]^T$ can be determined by chosen a first order dynamic behaviour with a time constant T = 1/k:

$$v_1 = k\,(y_{1c} - y_1), \; v_2 = k.(y_{2c} - y_2)$$

where, $y_c = [y_{1c}, y_{2c}]^T = [I_{dsc}, I_{qsc}]^T$ represents the reference stator current vector.

The block diagrams (Fig. 2) for the control of I_{ds} and I_{qs} can be summarized as follows:

The system transfer function obtained after decoupling and input-output linearization is P(s) Eq. 9:

$$P(s) = \frac{1}{1 + \tau s} \quad (9)$$

Fig. 1: Structure of the two new decoupled block diagram

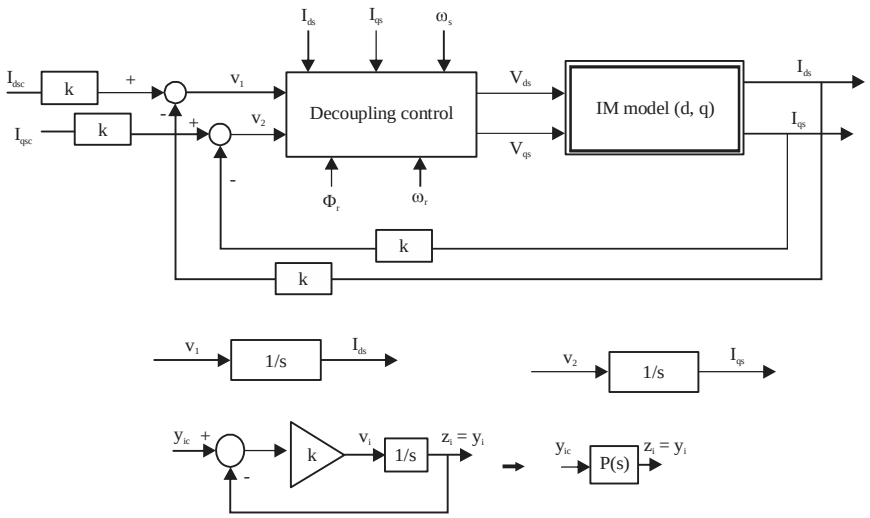

Fig. 2: Schematic diagram after decoupling, linearization and static looping

RESULTS AND DISCUSSION

Extensive simulations have been performed using Matlab/Simulink software[13] to examine the feedback control algorithms applied for 5.5 kW induction motor (Fig. 2). The nominal parameters of the induction motor are given in the Table 1. Note that, for simplicity and considerable rapidity, here we take t =10 msec, hence, $k = t^{-1} = 0.1$ msec.

Figure 3 shows the simulation of the system response with the nominal parameters of the IM (Table 1). Figure 4 gives the simulation results with the presence of the parametric variations (resistance or inductance variations).

From the Fig. 3, we can see a good regulation and uncoupling of the currents (I_{ds} and I_{qs}). The rise and descent phases of the current I_{qs} do not affect the output response of the current I_{ds}. In summary, in the nominal parameters case, the output values of currents converge very well to their reference values with a zero error.

In the non-nominal case (with at least 10% variation on the rotor resistance (R_{rn}) or inductance (L_{rn}), Fig. 4 shows a strong coupling between the currents because a step variation in I_{qs} generate a current I_{ds} change. Consequently, the currents reference waves are not quite similar to the output ones.

In short, from the Fig. 4, in order to assure a good regulation and convergence of the global system against parameter variations, it is necessary to build a robust current controller. In the following section, a strategy for a tracking robust regulator is analyzed.

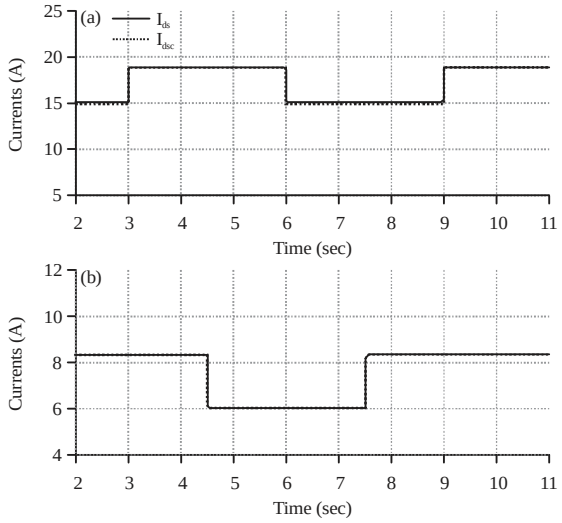

Fig. 3(a-b): Simulation response diagrams of currents in nominal case

Table 1: Nominal parameters of the induction motor

P_{mn} = 5.5 kW	Un = 220/380 V	In = 20.8/12 A	p = 2
Fn = 50 Hz	Wn = 1420 rpm	Jn = 0.005 kgN m^{-2}	fn = 0.012 Nm sec rad^{-1}
R_{sn} = 1 W	R_{rn} = 1.179 W	L_{sn} = 0.1197 H	L_m = 0.116 H
L_{fn} = 0.0037 H	L_{mn} = 0.116 H		

Robust control for the induction motor: In order to take into account the physical parameter variations and disturbances, a second loop using robust controller approach has been added on the IM drives (Fig. 5). This control algorithm uses H∞ synthesis[10,14] and "Doyle method"[11,12], to define robust controllers C(s) in order to realize the regulation of the currents and attenuate the disturbances.

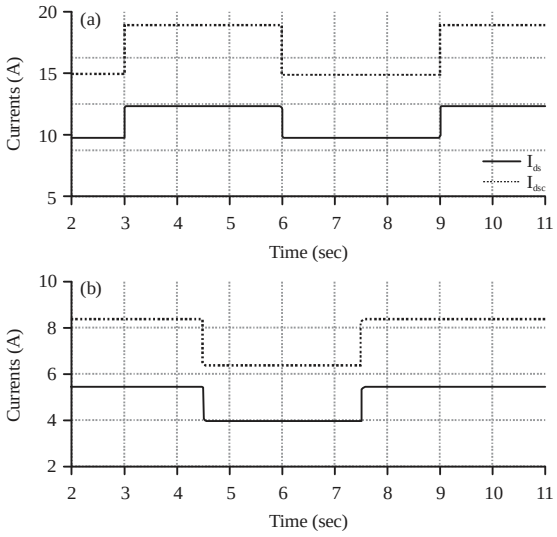

Fig. 4(a-b): Simulation response of currents under parameter variations ($R_r = 1.5R_{rn}$ and $L_r = 0.9L_{rn}$)

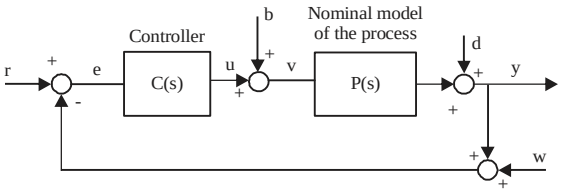

Fig. 5: A conventional representation of a closed-loop control scheme in the presence of measurement noises (w) and disturbances (b, d) affecting the control (u) and the process

From the block diagram of IM process Fig. 2 described by the stable transfer function P(s) after the linearization and static looping Eq. 8, the "Doyle" method applied on P(s) is given by the following lemma:

Lemma: By defining G, all stable transfer functions and clean. With an appropriate choice of a transfer function W(s), known as a Weighting function (WÎG), we have:

$$\lim_{\tau \to 0} \left\| W(s) \times (1 - J(s)) \right\|_{\infty} = 0$$

Where:

$$J(s) = \frac{1}{(1+\tau s)^{dr}} \text{ with } J(s) \in \Gamma$$

- For a transfer function $P(s) \in \Gamma$, the relative degree (d_r) of P(s) is:

d_r = (degree from denominator of P)-(degree from numerator of P), d_r>0

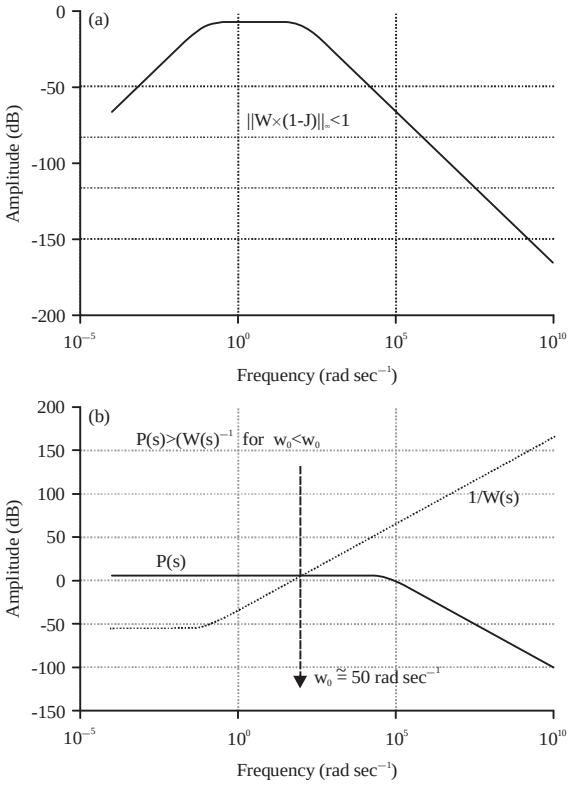

Fig. 6(a-b): "Doyle" method applied on the system P(s)

- The weighting function W(s) secures the performance of the closed loop system in order to minimize the tracking error ($e = y_c$-y), attenuate or reject noises (w) and disturbances (b, d) at low frequencies (up to a frequency = w_0)
- The real τ is an adjusting positive parameter, adequately chosen small (τ<1), in order to satisfy the robustness performance such as $||W\times(1-J)||_{\infty}<1$
- Thus, the robust controller synthesis is obtained by:

$$C(s) = J(s)P^{-1}(s)[1- J(s)]^{-1}$$

Thus, according to this "Doyle" lemma[11], in order to satisfy the robustness performance and stability for the IM process under parameters variation and disturbances, it can be defined a robust controller as follows:

- By using the "Bode" diagram (Fig. 6), for a frequency $w_0 \cong$ 50 rad sec^{-1}, a possible form of the weighting function W(s), such as W(s)>P(s), can be given by in Eq. 10:

$$W(s) = \frac{100}{2(s+0.09)} \quad (10)$$

which permits to reduce the static error and disturbances via the very small pole (s = -9.10)

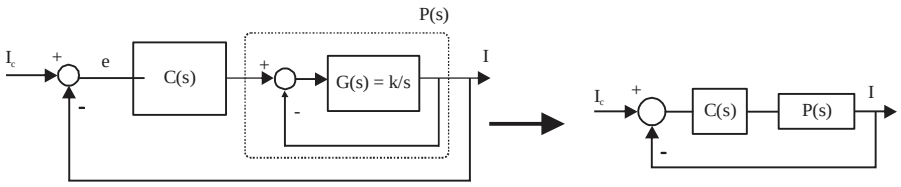

Fig. 7: Structural diagram of loop system in presence of the robust controller C(s)

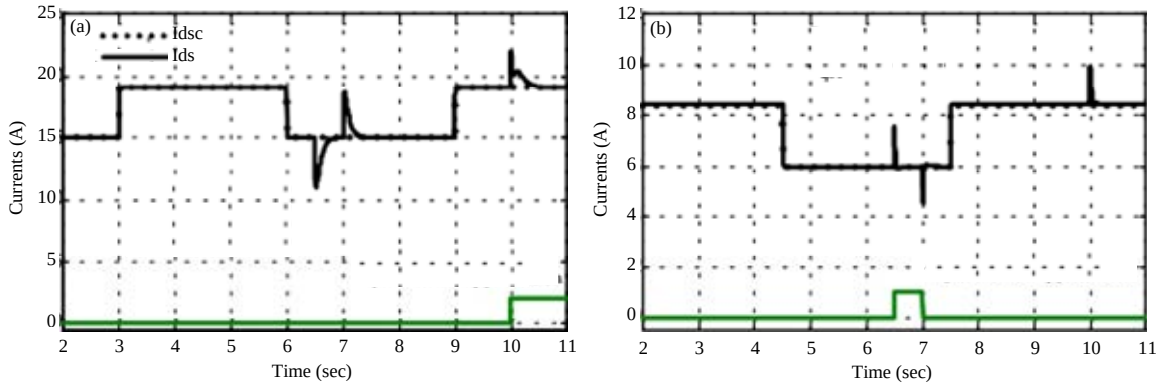

Fig. 8(a-b): Simulation results in the presence of the robust controller in nominal case

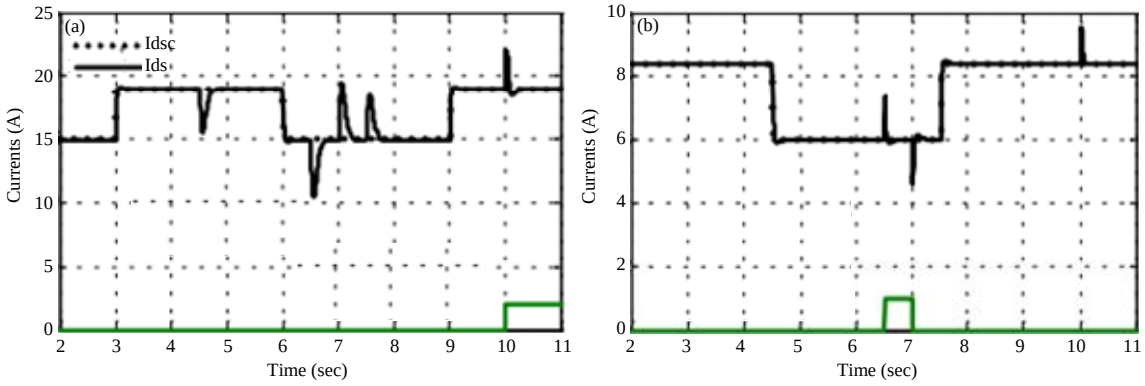

Fig. 9(a-b): Comparison of output currents responses and their reference values in the presence of the robust controller under disturbances and parametric variation ($\sigma_r = 1.5\ \sigma_{rn}$)

- We determine the relative degree value of P(s) : $d_r = 1$ and the real $\tau = 5$ msec chosen adequately small such as $||W \times (a\text{-}J)||_\infty < 1$; hence $J(s) = (1+\tau s)^{-1}$ all robust controller C(s), ensuring a good regulation and convergence of the stator currents of the IM system, may be written as Eq. 11:

$$C(s) = \frac{P^{-1}(s)J(s)}{1-J(s)} = 2\left(\frac{s+T^{-1}}{s}\right) \quad \text{with} \quad T = 10 \text{ msec} \qquad (11)$$

This robust controller C(s) is thus inserted into the control loop of our system P(s) as shown in the new bloc diagram structure given by the Fig. 7.

Simulations in presence of the robust controller: The performances and effectiveness of the robust controller C(s) as discussed, are analyzed by simulations carried out on the system described in Fig. 7.

Figure 8 and 9 show that the validity of the robust controller C(s) is demonstrated through the good simulation results in the presence of disturbances or parameter variations in IM. The static error between output currents responses and their reference values converges very well to zero and indicates that the currents tracking are achieved. Also, the disturbances are considerably reduced or disappear quickly on the currents dynamic behaviour. In other words, the stator

currents response is completely robust and stable with perfect rejection of disturbances despite changes in the rotor time constant (σ_r) value.

CONCLUSION

In summary, in order to assure a good decoupling, stability and suitable regulation of the stator currents, a robust feedback algorithm has been introduced and used for the control of an induction machine. Thus, the currents are regulated using a robust controller in the loop system based on the "Doyle" strategy and H∞ synthesis.

The interesting simulation results obtained on the induction motor show fast currents responses without overshoot and robust performance to parametric variation and disturbances in all the system.

Future work that comes naturally is the implementation in real-time, on a testing bench, of this proposed decoupling feedback control combined with a robust controller.

REFERENCES

1. Diyoke, G.C., C. Okeke and A. Uchechi, 2016. Different methods of speed control of three-phase asynchronous motor. Am. J. Electr. Electron. Eng., 4: 62-68.
2. Goyat, S. and R.K. Ahuja, 2012. Speed control of induction motor using vector or field oriented control. Int. J. Adv. Eng. Technol., 4: 475-482.
3. Vedrana, J., S. Zeljko and V. Zdravko, 2008. Optimal control of induction motor using high performance frequency converter. Proceedings of the 13th Power Electronics and Motion Control Conference, September 1-3, 2008, Poznan, Poland, pp: 705-709.
4. Saravanan, S. and K. Geetha, 2016. Single phase induction motor drive with restrained speed and torque ripples using neural network predictive controller. Circuits Syst., 7: 3670-3684.
5. Mansouri, M., H.N. Nounou and M.N. Nounou, 2014. Nonlinear control and estimation in induction machine using state estimation techniques. Syst. Sci. Control Eng., 2: 642-654.
6. Oteafy, A. and J. Chiasson, 2010. A study of the lyapunov stability of an open-loop induction machine. IEEE Trans. Control Syst. Technol., 18: 1469-1476.
7. Dendouga, A. and R. Abdessemed, 2015. Nonlinear feedback approach based on sliding mode controller for an induction motor fed by matrix converter. Courrier Savoir, 20: 21-30.
8. Zaidi, S., F. Naceri and R. Abdssamed, 2014. Input-output linearization of an induction motor using MRAS observer. Int. J. Adv. Sci. Technol., 68: 49-56.
9. Basilio, J.C., J.A. Silva, L.G.B. Rolim and M.V. Moreira, 2010. H∞ design of rotor flux-oriented current-controlled induction motor drives: Speed control, noise attenuation and stability robustness. IET Control Theory Applic., 4: 2491-2505.
10. Tety, P., A. Konate, O. Asseu, E. Soro, P. Yoboue and A.R. Kouadjo, 2015. A robust extended Kalman filter for speed-sensorless control of a linearized and decoupled PMSM drive. Engineering, 7: 691-699.
11. Doyle, J.C., B.A. Francis and A.R. Tannenbaum, 1992. Feedback Control Theory. 1st Edn., Maxwell MacMillan International, New York, USA., ISBN-13: 978-0023300110, Pages: 227.
12. Zhou, K. and J.C. Doyle, 1998. Essentials of Robust Control. Prentice-Hall, New York, USA., ISBN: 9780135258330, Pages: 425.
13. Gu, D.W., P. Petko and M.K. Konstantinov, 2013. Robust Control Design with MATLAB®. 2nd Edn., Springer, New York, USA., Pages: 468.
14. Li, J., H.P. Ren and Y.R. Zhong, 2015. Robust speed control of induction motor drives using first-order auto-disturbance rejection controllers. IEEE Trans. Ind. Applic., 51: 712-720.